VIII International Conference on Fracture Mechanics of Concrete and Concrete Structures
FraMCoS-8
J.G.M. Van Mier, G. Ruiz, C. Andrade, R.C. Yu and X.X. Zhang (Eds)

A SIMPLE TWO-STAGE MODEL FOR SIMULATING DRYING SHRINKAGE VS. MASS-LOSS EVOLUTION OF CONCRETE

A. DELAPLACE AND H. NOYALET

Lafarge Centre de Recherche
95, rue du Montmurier BP 15, 38291 Saint Quentin Fallavier Cedex, France
e-mail: arnaud.delaplace@lafarge.com

Key words: Drying process, mass loss, water content

Abstract. This paper presents a simple model aiming at simulating the drying shrinkage vs. mass-loss evolution of a concrete sample. It is based on a two-stage drying process. In a first stage, an external layer dries, as the central part of the sample has a fixed moisture. In a second stage, the central part of the sample dries. This simple model gives a reliable description of the drying process. The numerical results are compared to experimental ones, and we show that the model is able to predict the size effect of drying for standard concrete.

1 INTRODUCTION

Shrinkage of concrete results from different phenomena such as the hydration of cement or the self-dessication of the free water [1,2]. Concrete shrinkage has been widely studied as it can lead to unwanted cracking. Different models have been proposed, with different levels of complexity (see for example [3–6]). We propose in this paper a very simple model, based on a two-stage process. During the first stage, we assume that just a surrounding layer dries, leading to a fast loss of moisture in a thin layer. During the second stage, the center of the sample dries slowly to the equilibrium state that depends on the external relative humidity. This drying process is generally studied by recording the mass loss and the shrinkage evolution with respect to time. Modelling this evolution requires the knowledge of the diffusion coefficient as well as the convection properties. We limit our study to the evolution of the shrinkage with respect to the mass loss. The problem is considerably simplified as time is no more considered. Then, the proposed model just depends on four parameters, (i) the total moisture loss, (ii) the shrinkage coefficient, (iii) the thickness of the drying layer and (iv) the associated reduction of stiffness. For this first version of the model, we assume that the parameters are independent of the hydration level. This is a strong hypothesis but as we will see, it gives reliable results on standard concrete. After a presentation of the model and of the corresponding equations, the model is evaluated on different experimental results.

2 MODEL DESCRIPTION

The model is based on the observation that a drying shrinkage vs. mass-loss evolution reveals two stages for a wide varieties of concretes [7]:

- In a first part, a non linear evolution occurs, with a small average slope (O-A in figure 1);
- In a second part, a linear evolution with a high slope occurs until the equilibrium of the sample (A-B in figure 1).

Although different evolutions can be found for non standard concretes, this evolution is observed for standard cement pastes, mortars or concretes.

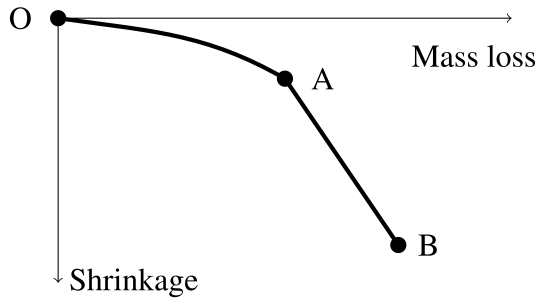

Figure 1: Schematics of the mass-loss versus drying shrinkage curve.

As this curve is not related to time, the explicit value of the diffusion coefficient and the boundary conditions are not used in the analysis. The model has just to describe the location of points O, A and B, and the evolution between these points. We propose next to explain the model behaviour on a 2D single-face drying sample.

2.1 First drying stage

In the initial state, the moisture of the sample is C_{ini} (figure 2-a). C_{end} will be the final one, and $\Delta C = C_{\text{ini}} - C_{\text{end}}$ is the total variation of moisture content during the drying process.

During the first stage, we assume that the moisture of the external face drops to the final value C_{end}. The thickness of the drying layer evolves from 0 to δ_1 (figure 2-b), and the moisture content is linear inside this layer. The center of the sample remains at the initial moisture content C_{ini}. During this evolution, the leading variable is the thickness δ of the layer, varying from 0 to δ_1. The final state of this first stage (figure 2-c) corresponds to point A in figure 1.

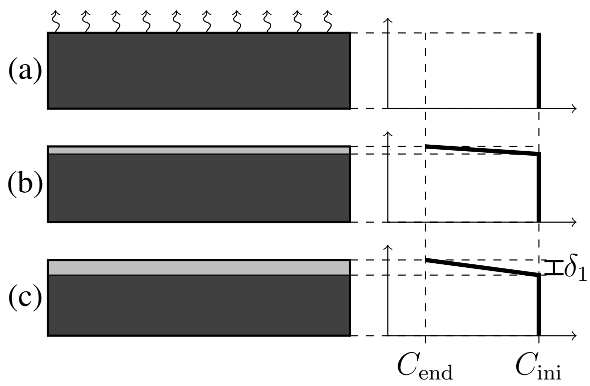

Figure 2: First drying stage: initial (a), intermediate (b) and final (c) states.

2.2 Second drying stage

During the second stage, the thickness of the external layer remains constant. The central part of the sample dries uniformly from C_{ini} to C_{end} moisture content (figure 3-d). The final state (figure 3-e) is a uniform moisture content C_{end}. During this second stage, the leading variable is the moisture content C of the central part.

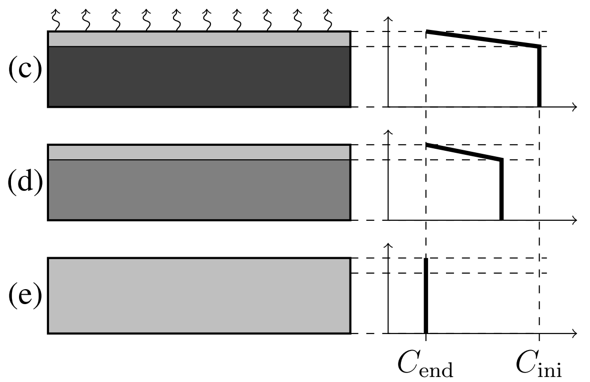

Figure 3: Second drying stage: initial (c), intermediate (d) and final (e) states.

2.3 Model parameters

The model depends on 4 parameters:

- ΔC, the variation of moisture,
- δ_1, the final thickness of the drying layer,
- κ, the shrinkage coefficient linking the variation of strain $\Delta\varepsilon_{sh}$ with the moisture variation $\Delta\varepsilon_{sh} = \kappa\Delta C$

- D, the coefficient that affects the stiffness in the drying layer. For our point of view, the origin of this reduction can be a cracking of the external surface [8, 9] or a skin effect (less aggregate in the drying layer).

3 APPLICATION ON A 6-FACE DRYING PRISMATIC SAMPLE

We propose in this section to establish the equations linking the drying shrinkage to the mass-loss. The following analysis can be extended to other geometries or other drying conditions.

A 6-face drying of a prismatic sample is considered. The length of the sample is ℓ, the cross section is a $p \times w$ rectangle. The total volume of the sample is $V_{tot} = \ell \times p \times w$. The volume of the central part is $V_c(\delta) = (\ell - 2\delta) \times (p - 2\delta) \times (w - 2\delta)$ where δ is the thickness of the drying layer. The volume of the drying layer is $V_e(\delta) = V_{tot} - V_c(\delta)$. In the same manner, the total area of a middle cross section is $S_{tot} = p \times w$, the central area is $S_c(\delta) = (p - 2\delta) \times (w - 2\delta)$ and the area of the drying layer is $S_e(\delta) = S_{tot} - S_c(\delta)$.

3.1 Mass-loss evolution

Stage 1

During this stage, the normalized mass-loss is simply:

$$\mu_1(\delta) = \frac{V_e(\delta)(C_{\text{ini}} - C_{\text{end}})/2}{M_0} \tag{1}$$

for $0 \leq \delta \leq \delta_1$. M_0 is the initial mass of the sample.

Stage 2

During the second stage, the mass-loss reads:

$$\begin{aligned} \mu_2(C) &= [V_e(\delta_1)(C_{\text{ini}} - (C_{\text{end}} + C)/2) \\ &\quad + V_c(\delta_1)(C_{\text{ini}} - C)] / M_0 \end{aligned} \tag{2}$$

for $C_{\text{end}} \leq C \leq C_{\text{ini}}$. Note that for $C = C_{\text{end}}$, we find the obvious relation for the total mass-loss $\mu_{\text{end}} = V_{tot}(C_{\text{ini}} - C_{\text{end}})/M_0$.

3.2 Shrinkage evolution

The shrinkage is evaluated considering a uniform distribution of the strain ε in the cross section, following the Euler-Bernoulli hypothesis (figure 4).

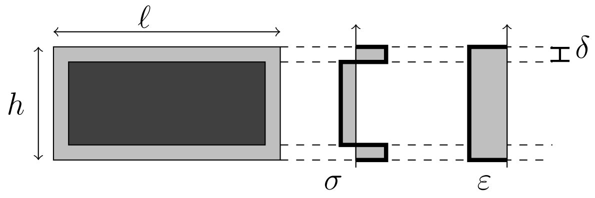

Figure 4: Stress and strain distribution in a central cross section.

Stage 1

The stress-strain relation reads:

$$\sigma = E(1 - D)\varepsilon_e \tag{3}$$

where E is the Young modulus of the central part, D is a variable that affects the Young modulus (typically due to cracking) and ε_e is the elastic strain expressed as:

$$\varepsilon_e = \varepsilon - \varepsilon_{sh} \tag{4}$$

where $\Delta\varepsilon_{sh} = \kappa \Delta C$ is the strain due to drying shrinkage and κ the shrinkage coefficient. For this study, the autogeneous, thermal and creep strains are neglected.

The force equilibrium in a central cross section is:

$$S_c(\delta)\sigma_c + S_e(\delta)\sigma_e = 0$$

with:

$$\sigma_c = E\varepsilon$$
$$\sigma_e = E(1 - D)\left(\varepsilon - \kappa\Delta C/2\right)$$

It leads to the following expression for the strain in the central part:

$$\varepsilon_{c_1}(\delta) = \frac{(1 - D)S_e(\delta)\kappa\Delta C/2}{(1 - D)S_e + S_c}$$

Additionnaly, one has to consider the uniform shrinkage of the left and right extremities:

$$\varepsilon_{ext_1} = \kappa\Delta C/2$$

and the total strain is:

$$\varepsilon_1(\delta) = \frac{(\ell - 2\delta)\varepsilon_{c_1}(\delta) + 2\delta\varepsilon_{ext_1}}{\ell} \tag{5}$$

Stage 2

The shrinkage of the extremities is:

$$\varepsilon_{ext_2} = \kappa \Delta C/2$$

The shrinkage of the central part is:

$$\varepsilon_{c_2}(C) = [(1-D)S_e\kappa(C_{\text{ini}} - (C_{\text{end}} + C)/2) + S_c\kappa(C - C_{\text{ini}})] / ((1-D)S_e + S_c)$$

and finally:

$$\varepsilon_2(C) = \frac{(\ell - 2\delta_1)\varepsilon_{c_2}(C) + 2\delta_1\varepsilon_{ext_2}}{\ell} \quad (6)$$

3.3 Parameters effect

The maximum abscissa of the global model response depends directly on the variation of moisture ΔC, as the maximum ordinate depends on the shrinkage coefficient κ. Figures 5 and 6 show the effects of δ_1 and of D on the global model response.

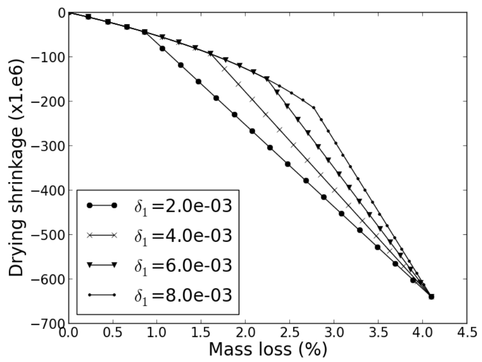

Figure 5: Effect of the surrounded drying layer thickness δ_1 ($\Delta C = 80$, $\kappa = 8. \times 10^{-6}$, $D = 0.80$).

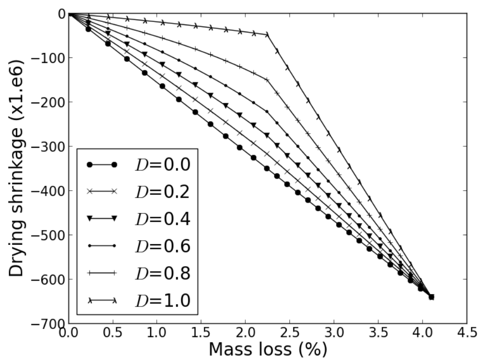

Figure 6: Effect of the stiffness reduction D of the drying layer ($\Delta C = 80$, $\kappa = 8. \times 10^{-6}$, $\delta_1 = 6. \times 10^{-3}$).

4 Experimental results

We propose in this part to apply this model on real experimental results. First, we explain the model parameters fitting for three different materials. Then, we analyse the ability of the model to predict the right behaviour with different boundary conditions.

4.1 Parameters fitting

The strategy to identify the parameters of the model is split in four parts:

1. Knowing the initial mass M_0 of the sample and the normalized final mass loss μ_{end}, the variation of moisture is:

$$\Delta C = \frac{M_0\mu_{\text{end}}}{V_{tot}} \quad (7)$$

where V_{tot} is the volume of the sample.

2. Knowing the final shrinkage $\Delta\varepsilon$, the shrinkage coefficient reads:

$$\kappa = \frac{\Delta\varepsilon}{\Delta C} \quad (8)$$

3. The thickness δ_1 of the external drying layer is obtained by fitting the abscissa of point A (figure 1).

4. Finally, the reduction of stiffness of the cracking layer is obtained by fitting the ordinate of point A.

4.1.1 Application to three concretes

This parameters identification has been applied on three different concretes with variable behaviours:

- a C25 concrete (C1)
- a lightweight concrete (C2)
- a concrete with a high W/C ratio (C3)

Figure 7 shows the experimental results and the best fitted curve for each concrete. One can see that a set of parameters can easily be identified from experimental results.

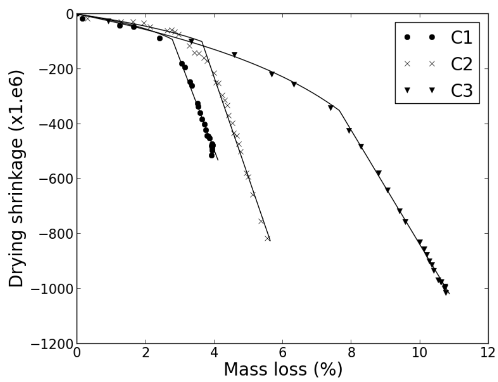

Figure 7: Identification of the model for three different concretes

Table 1 gives the corresponding values.

Table 1: Parameters values for the three concretes

	ΔC [kg/m^3]	$\kappa(\times 10^{-6})$ [m^3/kg]	D [-]	δ_1 [mm]
C1	77.	6.9	0.95	8.0
C2	55.	15.	0.98	7.5
C3	212.	4.8	0.82	8.5

One can see that whatever the material, the order of magnitude of δ_1 is closed to 8 mm, and D is closed to 1.

4.1.2 Size effect prediction

The model is pertinent if it has some prediction capabilities. We propose to assess this point on a set of prismatic samples. Different studies have shown the size effect on drying results [10, 11].

In our study, three sizes are used: $4 \times 4 \times 16$ cm, $7 \times 7 \times 28$ cm, $10 \times 10 \times 40$ cm samples. For all samples, a micro concrete is used. An additional size has been tested, a $2 \times 2 \times 16$ cm sample, but with mortar instead of the micro concrete. Although this is not the same material, we have included this sample in our comparison as the model doesn't take into account the microstructure of the material. For each size, two samples have been tested (filled and unfilled markers on figure 8).

The model parameters are identified on the $4 \times 4 \times 16$ cm sample. The values are: $\Delta C = 85$ kg/m^3, $\kappa = 6.8 \times 10^{-6}$ m^3/kg, $D = 0.88$ and $\delta_1 = 5.3$ mm. Figure 8 shows the experimental curves and the model prediction behaviour.

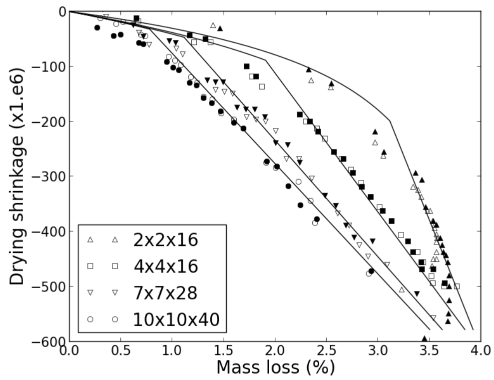

Figure 8: Prediction of the scale effect. Parameters are identified on the $4 \times 4 \times 16$ cm sample.

One can see that the model is able to predict in a reliable manner the evolution of shrinkage vs. mass loss for different sample sizes. These first results are encouraging and should be confirmed on different concrete formulations.

A second experimental campaign, with the same sample size but with different drying boundary conditions, is under progress and results will be presented during the conference.

5 CONCLUSIONS

A simple drying model is presented, aiming at representing the evolution of the shrinkage vs. mass loss evolution. As we want a simple model, some hypothesis have been done for the drying process:

- The drying process is assumed to be a two-stage process. In the first one, just a surrounding layer dries uniformly from the initial to the final water content value. In the second one, the center part of the sample dries uniformly.
- Four parameters control the drying process: the variation of water content, the

thickness of the surrounding layer, the shrinkage coefficient, the stiffness reduction in the surrounded layer.

We show that the model is able to reproduce the evolution of the shrinkage with respect to the mass loss for different types of concrete. More interestingly, the model is able to predict the size effect for a standard concrete. In this version, the model is not able to reproduce the effect of different hydration degree. It is one of the evolution we can consider for further developments.

REFERENCES

[1] Bažant, Z. P., Wittmann, F. H., 1982. *Creep and Shrinkage in Concrete Structures*, Chichester, John Wiley & Sons

[2] Hansen, W., 1987. Drying Shrinkage Mechanisms in Portland Cement Paste, *Journal of the American Ceramic Society*, **70**:323–328

[3] Wittmann, F. H. (1968), Surface tension shrinkage and strength of hardened cement paste, *Matériaux et Constructions*, **1**(6):547–552

[4] Xi, Y., Bažant, Z.P., Molina L., Jennings, H.M. (1994), Moisture diffusion in cementitious materials: moisture capacity and diffusivity, *Advanced Cement Based Materials*, **1**:258–266

[5] Torrenti, J.M., Granger, L., Diruy, M., Genin, P. (1997) Modeling concrete shrinkage under variable ambient conditions, *ACI Mater. J.*, **96**(1):35–39

[6] Mu, R., Forth, J.P. (2009) Modelling shrinkage of concrete from moisture lost using moisture diffusion theory, *Magazine of Concrete Research*, **61**:491–497

[7] Bakhshi, M., Mobasher, B., Soranakom, C. (2012) Moisture loss characteristics of cement-based materials under early-age drying and shrinkage conditions, Construction and Building Materials **30**:413–425

[8] Bažant, Z.P., and Raftshol, W. J. (1982). Effect of cracking in drying and shrinkage specimens. *Cement and Concrete Research*, **12**:209–226;

[9] Bisschop, J., Wittel, F. (2011) Contraction gradient induced microcracking in hardened cement paste, *Cement & Concrete Composites*, **33**:466-473

[10] Almudaiheem, J. A., Hansen, W. (1987) Effect of Specimen Size and Shape on Drying Shrinkage, *ACI Materials Journal*, **84**:130–135

[11] Al-Saleh, S.A., Al-Zaid, R.Z., (2006) Effects of Drying Conditions, Admixtures, and Specimen Size on Shrinkage Strains, *Cement and Concrete Research*, **36**:1985–1991